

Fluctuating Pressure Inside/Outside the Flow Separation Region in High Speed Flowfield

Zhao Lei, Zhao Xiaojian and Li Suxun

CAAA (China Academy of Aerospace Aerodynamics), Beijing 100074, China

Received: December 02, 2014 / Accepted: December 12, 2014 / Published: January 30, 2015.

Abstract: An experimental study was conducted on the interactions of shock wave/turbulence or laminar boundary layer caused by fin-type protuberance, as the lack of detailed understanding of fluctuating pressure loads inside and outside the laminar or turbulence boundary layer separation region in hypersonic flow. The changes of fluctuating pressure in separation region were focused on in this paper. The study shows that the existence of fin changes flowfield on the plate significantly. The laminar boundary layer separation occurs earlier and the separation region is more extensive. Similar flow is observed between a couple of measurement points outside the laminar separation region. However, there are significant differences between the flow inside and outside the separation region. The level of fluctuating pressure of laminar boundary layer is smaller than that in turbulent case. Even so, in laminar case, the peak fluctuating pressure still reaches a high level. Therefore, the structural influence (damage and/or early fatigue) of fluctuating pressure loads caused by the laminar boundary layer separation should not be ignored.

Key words: Hypersonic separated flow, laminar flow, blunt fin, fluctuating pressure.

1. Introduction

The severe unsteady aerodynamic/aerothermal loads associated with shock wave/boundary layer and shock/shock interaction can affect the performance and security of hypersonic vehicles. As early as the World War II, researchers have been engaged in studies to understand and predict corresponding problems in supersonic and even hypersonic flows of high-speed aircrafts and missiles. Over the past decades many experimental and computing studies have been performed on this topic. A detailed review of recent works was presented by Clemens and Narayanaswamy [1]. Even though the physical mechanisms of SWBLI (shock wave/boundary layer interaction) are still not quite clear. For example, what drives the shock movement velocity? Is the driving mechanism of low-frequency unsteadiness forced by the upstream turbulent boundary layer, or is it due to the intrinsic instability of the separated flow? Dolling

and Brusniak [2] has performed extensive studies on SWBLI in hypersonic flow ($M_\infty = 5$), and summarized some of the key questions [3] that computations and further experiments should be addressed.

Most of the existing studies focus on the SWTBLI (shock wave/turbulent boundary layer interaction). However, for much larger flight velocity and higher flight altitude of advanced vehicles, especially for hypersonic vehicles with lifting body, SWLBLI, often accompanied by separation, is a ubiquitous feature of vehicles. Laminar boundary layer separation induced by the disturbance occurs easier than turbulent case. Study of SWLBLI has become the actual engineering requirement, and become urgent increasingly.

An experimental study was conducted on the interactions of shock wave/turbulence or laminar boundary layer caused by fin-type protuberance, as the lack of detailed understanding of fluctuating pressure loads inside and outside the laminar or turbulence boundary layer separation region in hypersonic flow. The changes of fluctuating pressure in separation region were focused on in this paper.

Corresponding author: Zhao Lei, master, research field: fluid mechanics. E-mail: zhaole0706@gmail.com.

2. Experimental Setup and Methods

2.1 Wind Tunnel

The experiments were performed in FD-20 hypersonic gun tunnel of CAAA (China Academy of Aerospace Aerodynamics), in which the axis symmetrical nozzle exit is Φ 480 mm. Experiments were performed under such conditions as Mach number 6, Reynolds number $Re = 15 \times 10^6/\text{m}$ and $40 \times 10^6/\text{m}$ (turbulence separated flowfield), and as Mach number 8, Reynolds number $Re = 8 \times 10^6/\text{m}$ and $40 \times 10^6/\text{m}$ (laminar separated flowfield). The typical stable flow period was about 20 milliseconds.

2.2 Test Model

A model with a plate/blunt swept fin configuration was employed. The dimensions for the flat plate were 680 mm (length) \times 380 mm (width) and the sharp leading edge angle was 10° . The boundary layer was developed from the leading edge of the flat plate. Sweep angle of the fin was selected at $\Lambda = 45^\circ$. The semi-cylindrical leading edge of the fin had a diameter of $D = 25$ mm. The distance between the leading edge of the flat plate and the fin was 432.5 mm. The fin was placed normal to the flat plate (Fig. 1).

The origin of the coordinate system is located in the intersection point of the leading edge of the fin and the centerline of the flat plate, as shown in Fig. 2. OX axis points to downstream along with the centerline of the flat plate. OS axis points to the top of fin along with the leading edge of the fin. The model was supported by a sting in the test section.

2.3 Instrumentation and Data Acquisition

The detailed surface fluctuating pressure distributions in the interaction regions on the flat plane and the leading edge of the fin were measured. For the requirement of space resolution, two types of Kulite transducers, whose diameters were 2.4 mm and 1.6 mm respectively, were employed for the fluctuating pressure measurement. The minimum distance between two transducers was 3 mm.

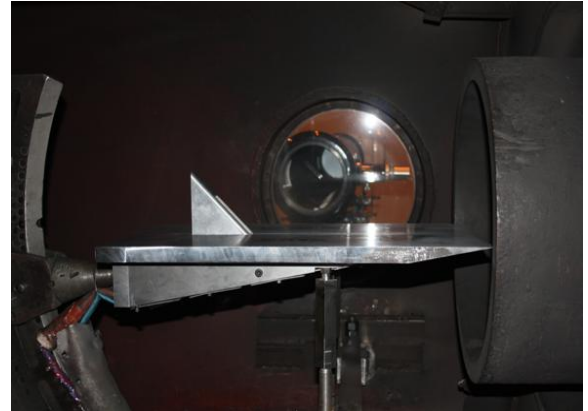


Fig. 1 Model setup.

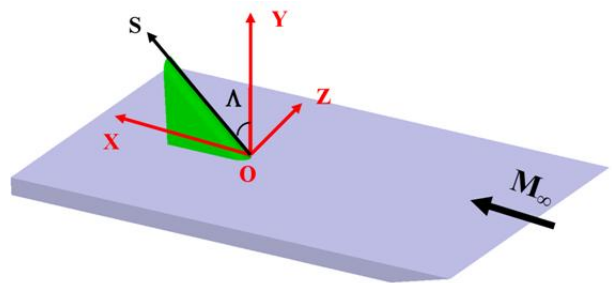


Fig. 2 Coordinate system.

Atria total pressure (P_0) triggered the instrument operation. The fluctuating pressure signals derived from the transducers were modulated and amplified by the SDY-2107B filter, and then was acquired simultaneously by the VXI-16026A data acquisition system with 200 ksps for each channel and downloaded to a PC. The classical sample acquisition time is 20 milliseconds.

High speed schlieren video with 2,000 frames per second was also taken to visualize the time-varying structure of the separated flow.

2.4 Test Conditions

The experimental conditions are shown in Table 1. All the experimental test conditions were repeated three times in order to get creditable results.

Under these conditions, it is known from the previous study Ref. [4] that the boundary on the plate ahead of the fin was laminar for Mach number 8.0, and turbulent for Mach number 6.0. It should be noticed that, the boundary was close to transition for $M_\infty = 8.0$ and $Re = 33.8 \times 10^6/\text{m}$ case.

Table 1 Test conditions.

Run	M_∞	P_0/MPa	T_0/K	$Re/\text{m}^{-1}(\times 10^6)$
1,376	8.0	6.55	1,093	7.77
1,378	8.0	16.76	788	33.8
1,382	6.0	3.37	818	13.0
1,384	6.0	9.97	900	33.2

2.5 Data Post Processing

The statistical approach was employed for random signals analysis. Total pressure of the gun tunnel existed fluctuation due to its operating mode. The fluctuating pressure signal was not proper stationary random process. This characteristic will lead to a considerable statistical error when using traditional statistical approach. Assume that all measured signals change with total pressure fluctuation, and the multivariate linear regression analysis algorithm can be used to get the signal offsets due to total pressure fluctuation. Deducting the offsets from the raw signals and then a quasi-stationary random process can be gotten. The method significantly improved the experimental repeatability and the maximum measured deviation decreased to less than 5 dB.

The analysis data included fluctuating wall pressure distributions, spectrum and correlation functions of measurement points.

The total SPL (sound pressure level) of the measured fluctuating pressure is defined as:

$$\text{SPL} = 20 \log_{10} \frac{p_{rms}}{p_{ref}} \quad (1)$$

where, $P_{rms} = \left[\sum_{i=1}^N (p_{wi} - \bar{p}_w)^2 \right]^{1/2}$ is the root-mean-square pressure, and the reference pressure is $p_{ref} = 2 \times 10^{-5} \text{ Pa}$.

Welch method, which can decrease statistical variance deriving from discrete Fourier transform, was employed for the spectral analysis. The power spectral densities were computed by segmenting data, each segment with a transform length of 2,048 points. A Hanning window with 50% overlap was used for averaging to get a reliable estimate of the spectra. The

frequency resolution obtained after performing FFT (fast fourier transform) on each segment was 97.65 Hz. The maximum analysis frequency was 10 kHz.

The cross-power spectral density function between two measured points is defined as:

$$G_{ij}(f) = \frac{1}{MN_{\text{FFT}}} \sum_{k=1}^M P_i^{k*}(f) P_j^k(f) \quad (2)$$

where, $P_i^k(f)$ is the Fourier transform of the k th block of the signal at transducer i . $*$ indicates complex conjugate. The spectral has been averaged overtime M blocks. Self-power spectral density function corresponds to $i = j$. Cross-correlation function $r_{ij}(\tau)$ is the inverse Fourier transform of the cross-power spectral density function $G_{ij}(f)$.

3. Results and Discussion

3.1 Structure of Flow Field

The typical flowfield of blunt fin induced separated flow is visualized by the schlieren photography as shown in Fig. 3. An upstream shock wave is formed induced by the blunt fin. It brings the converse pressure gradient. Disturbance transfers towards upstream through the subsonic region of the boundary layer, which causes separated flow. The oblique separation shock eventually connects with the detached shock wave of the blunt fin, and forms complex λ shock wave systems. An oscillating separation shock can be observed from the schlieren video. The unprecise estimate oscillating frequency of laminar flow is about 500 Hz. It cannot be estimated for turbulent case due to over narrow separation region. It shows that the laminar boundary layer separation occurs earlier and the separation region is more extensive. Based on the scale calibration of the schlieren photo, it can be estimated that: (1) the laminar boundary layer separation started on the upstream of fin at about $X/D \approx -2.0$ (on the plate), the laminar reattached point was at about $S/D \approx 0.38 \sim 0.5$ (on the fin). (2) for turbulent case, $X/D \approx -0.4$ and $S/D \approx 0.38$, respectively.

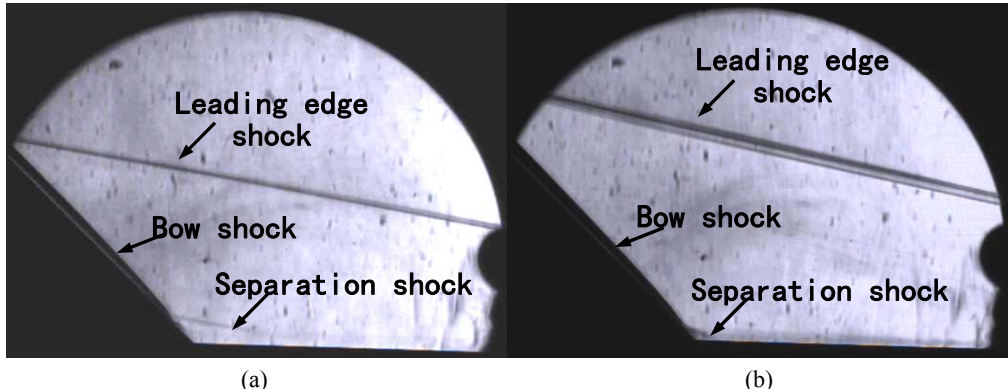


Fig. 3 Schlieren photo of (a): the laminar interactive flow, $M_\infty = 8.0$, $Re = 7.77 \times 10^6/\text{m}$; (b): the turbulent interactive flow, $M_\infty = 6.0$, $Re = 33.2 \times 10^6/\text{m}$.

3.2 Distributions of Fluctuating Pressure

Fluctuating pressure distributions along the centerline of the plate/fin model are shown in Fig. 4. The dashed line indicates the distributions on a flat plate (without disturbance) model. The solid line indicates the distributions on a plate/blunt swept fin (with disturbance) model.

For the results in the “without disturbance” cases, fluctuating pressure distributions display a horizontal shape, whether the boundary is laminar, turbulent or transitional case. In fact, it indicates the wind tunnel background noise of the attached flow on the plate. The low-level fluctuating pressure signals are covered by the background noise. For this reason, the process of flow transitional cannot be captured here.

The study shows that the existence of fin changes flowfield on the plate significantly [5]. The blunt swept fin induces the upstream boundary layer separation. The shock impinging point formed by the upstream separate shock and the bow shock is on the leading edge of the fin. Flow is reattached here. The fluctuating pressure distributions on a flat plate showed a highly complex region which corresponded to the separation region. Significant differences are noted in the fluctuating pressure distributions of laminar boundary layer separation with that of turbulent case. The fluctuating pressure in the laminar case reaches about 120 dB on the flat plate. The

boundary layer separation starts on the upstream of fin at about $X/D \approx -2.0$ (on the plate). And the maximum peak pressure reaches about 170 dB on the leading edge of the fin, which occurs at the impinging triple point $S/D = 0.5$. On the other hand, the fluctuating pressure in the turbulent case reaches about 140 dB on the flat plate. The boundary layer separation region is limited in the small junction of the blunt fin and the flat plate, and correspondingly initial separation position is at $X/D = -0.42$ (adjacent to the fin, on the plate). The observed peak pressure is at about $S/D = 0.38$ with about 190 dB. The measured values of the separation region agree with the estimated values from the schlieren photos (Section 3.1). It implicates that, (1) the fluctuating pressure in the turbulent case is much larger than that in the laminar case; (2) the laminar boundary layer separation occurs earlier and the separation region is more extensive.

It should be noticed that, in the $M_\infty = 8.0$ and $Re \approx 40 \times 10^6/\text{m}$ cases, the measured initial separate positions were different between various test runs depend on the local boundary layer condition (Fig. 5). It represented laminar feature for $Re = 37.8 \times 10^6/\text{m}$ case, which the initial separation position is at $X/D \approx -2.0$. On the other side, turbulent feature was shown for $Re = 33.8 \times 10^6/\text{m}$ case, which the initial separation position is at $X/D \approx -0.5$. It is considered that, the boundary layer ahead of the blunt fin is close to transition, when free flow $M_\infty = 8.0$ and $Re \approx 40 \times 10^6/\text{m}$ [4]. The unsteady

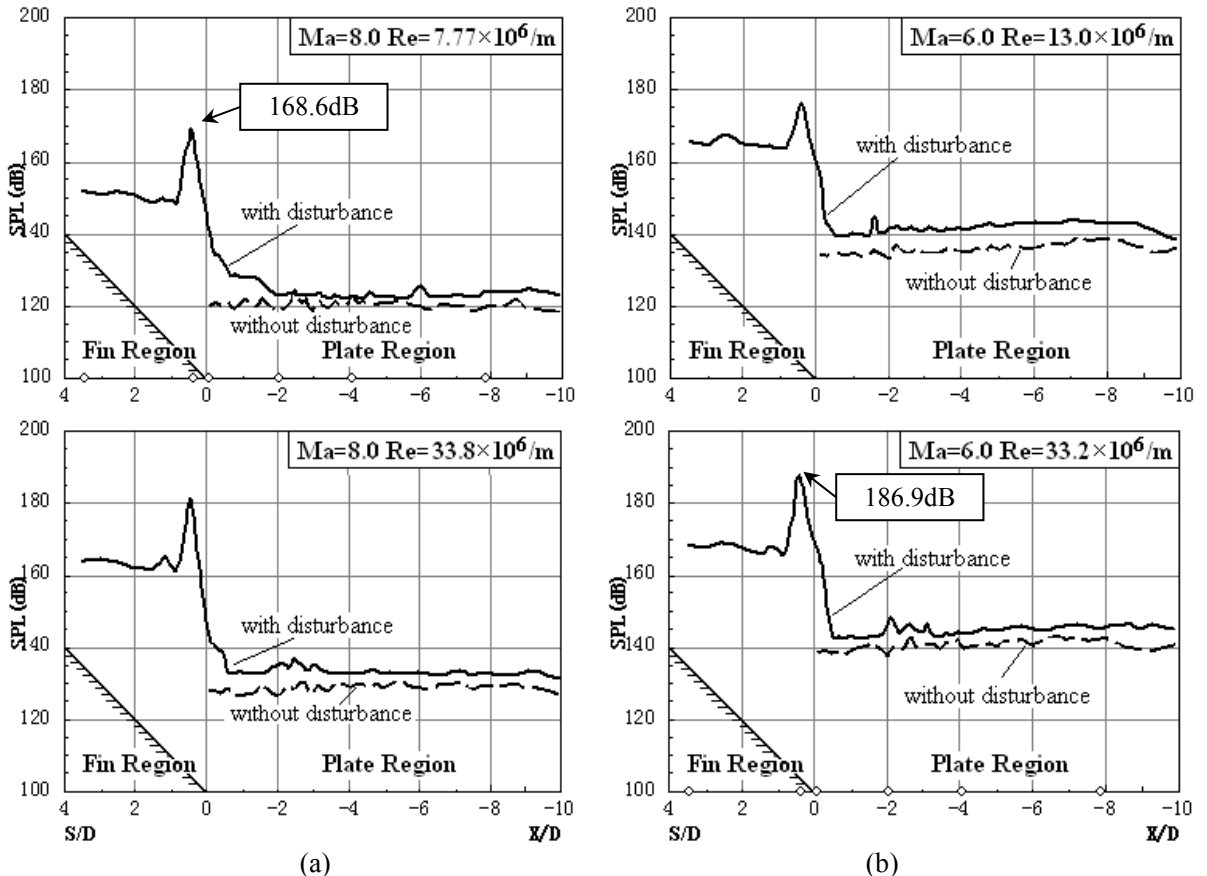


Fig. 4 Fluctuating pressure distribution along the centerline of the plate/fin model. (a): laminar boundary layer; (b): turbulent boundary layer.

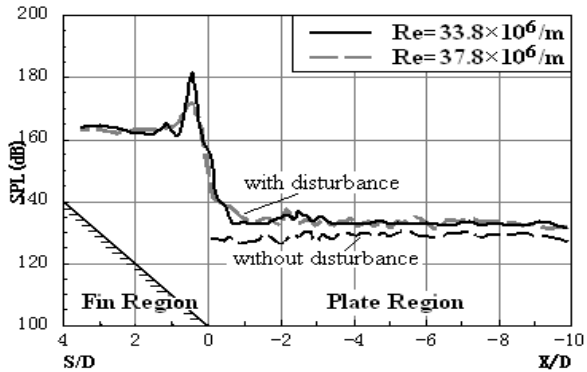


Fig. 5 Fluctuating pressure distribution for the transitional boundary layer ($M_\infty = 8.0$, $Re \approx 40 \times 10^6/m$).

transition affects the flow separation. The peak fluctuating pressure difference was produced by different measurement points arrangements and transducers with different diameters were employed between two cases.

For contrasting the laminar with turbulent flow, two classical test conditions were selected: (1) $M_\infty = 8.0$,

$Re = 7.77 \times 10^6/m$ for the flat plate model and for the laminar flow, (2) $M_\infty = 6.0$, $Re = 33.2 \times 10^6/m$ for the turbulent flow. The typical measurement points (circles on the x-coordinate in Fig. 4) corresponding to various boundary layer conditions are shown in Table 2.

Significant differences are noted in the fluctuating pressure random characteristics between laminar and turbulent flow (Fig. 6). Attached flow develops from the leading edge of the flat plate. In the laminar case, fluctuating signal is unobservable from upstream of

Table 2 Typical measurement points.

Position	Laminar	Turbulence
$X/D = -7.8$	Attached flow	Attached flow
-4.08	Attached flow	Attached flow
-2.0	Start separate	Attached flow
-0.1	Separated flow	Separated flow
$S/D = 0.38$	Near reattach	Near reattach
3.5	Attached flow	Attached flow

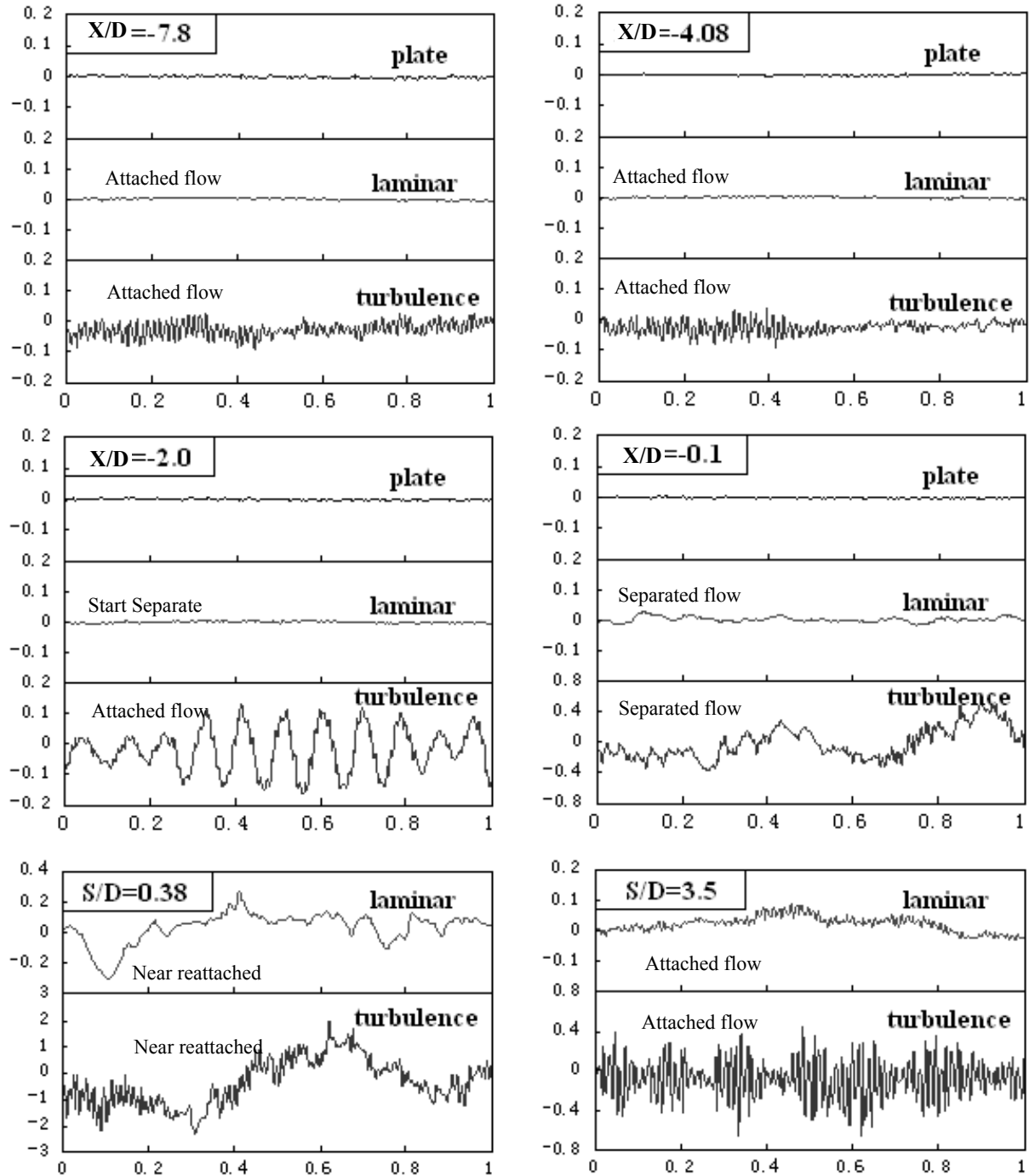


Fig. 6 Typical time domain signals.

Plate/laminar: $M_\infty = 8.0$, $Re = 7.77 \times 10^6/\text{m}$; turbulence: $M_\infty = 6.0$, $Re = 33.2 \times 10^6/\text{m}$.

the fin, and observed slight fluctuating signal is from the junction of the blunt fin. However, clear fluctuating signal is observed even from the far upstream of the fin for the turbulent case. It indicates that the fluctuating pressure of turbulence is clearly larger than that in the laminar case. The fluctuating

pressure load grows remarkably downstream the flow separation. For both of laminar and turbulent cases, the maximum fluctuating pressure position is at the reattached point on the leading edge of the fin. It also shows that the energy of high frequency band increases gradually along with the flow direction.

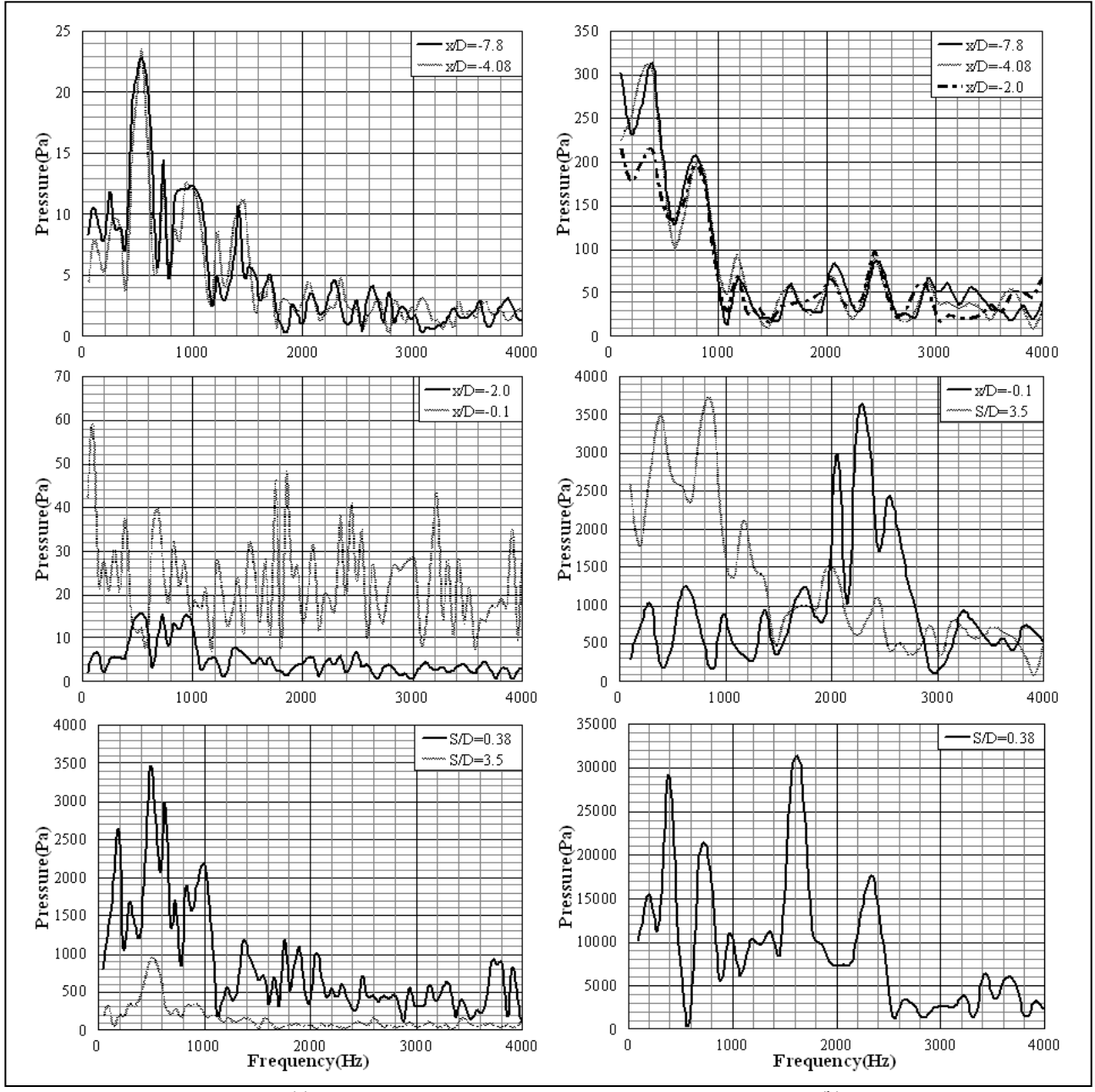


Fig. 7 Typical frequency domain signals. (a): Laminar, $M_\infty = 8.0$, $Re = 7.77 \times 10^6/\text{m}$, oscillating frequency $f = 500 \text{ Hz}$; (b): turbulence: $M_\infty = 6.0$, $Re = 33.2 \times 10^6/\text{m}$, oscillating frequency $f = 400/700 \text{ Hz}$.

Oscillating frequencies obtained from fluctuating pressure signals are baseline frequency, which is lower than 1 kHz, and its octaves (Fig. 7). The observed oscillating frequency of laminar flow is about 500 Hz, agreeing with the estimate value from the schlieren video. It is about 400 or 700 Hz for the turbulent case. They are agreeing with the results of

unsteady heat flux measurement [6]. The value of peak spectral line in the turbulent case is about 10 times larger than that of laminar case. The spectral lines in the turbulent case are much more than that of laminar case.

Typical correlation functions are shown in Fig. 8. It can be seen that, there is some correlation between a

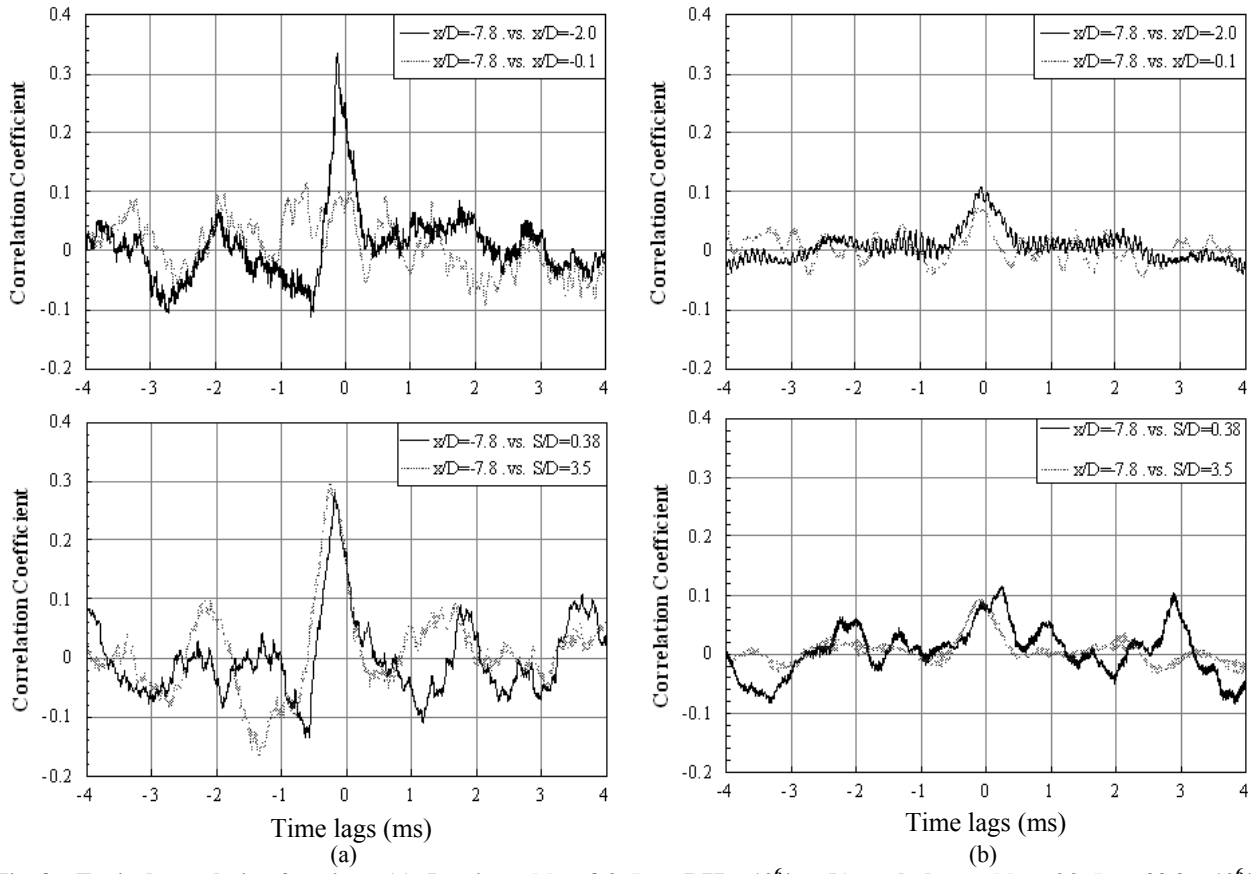


Fig. 8 Typical correlation functions. (a): Laminar, $M_\infty = 8.0$, $Re = 7.77 \times 10^6/\text{m}$; (b): turbulence: $M_\infty = 6.0$, $Re = 33.2 \times 10^6/\text{m}$

couple of measurement points outside the laminar separation region, whose peak correlation is about 0.3. Therefore, similar peak frequencies can be observed in the spectrum (Fig. 7). However, the correlation is weak between a point inside the separation region and an outside one. It indicates that there are significant differences between the flow inside and outside the separation region. On the other hand, the correlation is usually weak between arbitrary two measured points in turbulent case, whose peak correlation is only about 0.1, wherever they are inside or outside the separation region. It can be considered as determined by the disordered state of the turbulence.

It is also noted that the fluctuating wall pressure increases as Reynolds number grows up. It is observed that the level of fluctuating pressure of laminar boundary layer is about 15~20 dB smaller than that in turbulent case throughout the testing (Fig. 4). Even so,

in laminar case, the peak fluctuating pressure still reaches about 170 dB. Therefore, the structural influence (damage and/or early fatigue) of fluctuating pressure loads caused by the laminar boundary layer separation should not be ignored.

4. Conclusions

Previously, few studies focused on SWBLI of which Mach number $M_\infty > 5$. Specially, the characters of SWBLI have not been known yet. In this paper, an experimental investigation of the separated flow characteristics caused by a $\Lambda = 45^\circ$ swept blunt fin on the flat plate in hypersonic laminar/turbulent flow was carried out. The detailed surface fluctuating pressure was measured. Schlieren pictures of the fin shock wave were taken. Significant differences are noted in the fluctuating pressure random characteristics between laminar and turbulent flow. The following

conclusions can be drawn:

The existence of the fin changes flowfiled on the plate significantly. There is a highly complex disturbance region upstream of fin. Significant unsteady pressure loads are observed.

The blunt fin with 45° swept angle induces the boundary layer separation. The separation shock impacts the leading edge of the fin, then the flow reattach. Disturbance transfer towards upstream through the subsonic region of the boundary layer. A shock wave oscillation occurs. Fluctuating pressure reaches peak value at the reattached point on the leading edge of the fin.

The disturbance resistance of the laminar boundary layer is poor than that of turbulent case. The laminar boundary layer separation occurs earlier and the separation region is more extensive.

Similar flow is observed between a couple of measurement points outside the laminar separation region. However, there are significant differences between the flow inside and outside the separation region in laminar or turbulent cases.

The level of fluctuating pressure of laminar boundary layer is smaller than that in turbulent case. Even so, in laminar case, the peak fluctuating pressure still reaches a very high level, and should not be ignored.

Acknowledgements

The authors acknowledge the support from the Key National Natural Science Foundation of China (No. 91116009 & No. 91216114). The support provided by the FD-20 wind tunnel staff is greatly appreciated.

References

- [1] Clemens, N. T., and Narayanaswamy, V. 2009. "Shock/Turbulent Boundary Layer Interactions: Review of Recent Work on Sources of Unsteadiness." *AIAA 2009-3710*.
- [2] Dolling, D. S., and Brusniak, L. 1994. *Flowfield Dynamics in Blunt Fin-Induced Shock Wave/Turbulent Boundary Layer Interactions*. Final report. N1994-27802.
- [3] Dolling, D. S. 2001. "Unsteadiness of Shock-Induced Turbulent Separated Flows—Some Key Questions." *AIAA 2001-2708*.
- [4] Li, S. X., and Guo, X. G. 2010. "Blunt Fin Induced Shock Wave/Laminar and Transitional Boundary Layer Interaction in Hypersonic Flow [C]." Proceedings of the 13th Asian Congress of Fluid Mechanics, Dhaka, December 2010.
- [5] Li, S. X., Shi, J., and Guo, X. G. 2014. "Experimental Study of the Boundary Layer Features on a Flat Plate in High Speed Flow." In *4th International Conference on Experimental Fluid Mechanics*.
- [6] Ma, J. K., and Li, S. X. 2014. "Heat Flux Measurement in Separated Flowfield Induced by a Swept Blunt Fin." In *4th International Conference on Experimental Fluid Mechanics*.